

A Comprehensive Comparison of Different Control Strategies to Adjust the Length of the Soft Contractor Pneumatic Muscle Actuator

Heba Ali Al-Mosawi*, Alaa Al-Ibadi, Turki Y. Abdalla

Computer Engineering Department, College of Engineering, University of Basrah, Basrah, Iraq

Correspondence

* Heba Ali Al-Mosawi
Computer Engineering Department, College of Engineering,
University of Basrah, Basrah, Iraq
Email: engpg.heba.ali@uobasrah.edu.iq

Abstract

According to the growing interest in the soft robotics research field, where various industrial and medical applications have been developed by employing soft robots. Our focus in this paper will be the Pneumatic Muscle Actuator (PMA), which is the heart of the soft robot. Achieving an accurate control method to adjust the actuator length to a predefined set point is a very difficult problem because of the hysteresis and nonlinearity behaviors of the PMA. So the construction and control of a 30 cm soft contractor pneumatic muscle actuator (SCPMA) were done here, and by using different strategies such as the PID controller, Bang-Bang controller, Neural network controller, and Fuzzy controller, to adjust the length of the (SCPMA) between 30 cm and 24 cm by utilizing the amount of air coming from the air compressor. All of these strategies will be theoretically implemented using the MATLAB/Simulink package. Also, the performance of these control systems will be compared with respect to the time-domain characteristics and the root mean square error (RMSE). As a result, the controller performance accuracy and robustness ranged from one controller to another, and we found that the fuzzy logic controller was one of the best strategies used here according to the simplicity of the implementation and the very accurate response obtained from this method.

KEYWORDS: Soft Robots, Soft Contractor Pneumatic Muscle Actuator(SCPMA), Control System, PID, Bang-Bang, Neural Network, Fuzzy.

I. INTRODUCTION

Inspired by nature, engineers began to explore the design and control of flexible robots made from compatible materials, so, we can define soft robots as systems capable of autonomous behavior and consist primarily of materials similar to Biological materials. Softness and compliance with the body are notable features often exploited by biological systems, which tend to seek simplicity and show less complexity in their interactions with the environment. the rigid robots control movements can be described by six degrees of freedom (three translations about the x, y, and z axes and three rotations), while the motions of soft robots cannot be limited to planar movements, due to the flexibility of the soft materials; it can twist, bend, buckle, compress, wrinkle, stretch, etc. these moves can be considered as offering infinite degrees of freedom [1]. The emergence of soft robots brings new opportunities to the field of robotics, as they can adapt to unstructured environments, especially those with uncertainty and human-robot interactions. Accuracy and efficiency have always been internal

motivators for the development of rigid robots, which have been widely used in industrial automation. In contrast, soft robots are more difficult to precisely design than rigid robots, so their control accuracy and efficiency cannot be compared to rigid robots, and as a result, soft robots may not be applicable in industrial automation, so there is no need to exaggerate accuracy and efficiency, especially in the early stages of soft robotics. Aside from that, all robotics theories and techniques should be mainly focused on application. So, in terms of control, the controller that meets current needs can be used to investigate new applications and can be improved later based on specific problems [2]. Particularly in soft robots, new algorithms and techniques were needed to differ from that of rigid robots, and the control complexity of the system model was increased due to nonlinearity and hysteresis in the soft robot behavior; the nonlinear behavior is due to the viscoelastic properties of the internal bladder, the air pressure, the structure and complex behavior of the outer braided sleeve covering the PMA, while the hysteresis behavior is due to the internal bladder, which results in a



This is an open access article under the terms of the Creative Commons Attribution License, which permits use, distribution and reproduction in any medium, provided the original work is properly cited.

© 2022 The Authors. Published by Iraqi Journal for Electrical and Electronic Engineering by College of Engineering, University of Basrah.

different performance of the PMA under different pressure conditions [3]. Artificial muscles are made of materials of variable stiffness, and the stiffness of pneumatic artificial muscles is directly proportional to the compressed air inside them [4].

Soft robots have been used extensively in numerous areas, especially in the last two decades. So researchers from different fields such as material science, biology, and computer and control engineering were interested in the soft robotics field and its control [5], from these studies, the designing of the three fingers gripper from the self-bending contraction actuator, and the extension-circular gripper made from the extension PMA and the contraction PMA for A. Al-Ibadi *et al* [6], the author proposed a self-bending contraction actuator and uses it in the designing of the two grippers, the control system used was a neural network controller, which is NARMA-L2 model to control the required grasping force according to the object weight. Also, a single actuator continuum robot arm with a two-fingers soft gripper has been designed from the self-bending contraction actuator (SBCA), which offers significant assistance to humans in preventing or reducing pain caused by bending the human back [7]. while J. Hao *et al* [2] proposed Honeycomb pneumatic networks (HPN) which are derived from embedded pneumatic networks (EPN), the name comes from the shape that resembles a honeycomb chamber in a hexagonal structure, HPN is an elastic structure, and its deformation is mainly due to the changing in the angle between the honeycomb chambers walls rather than the deformation in the used materials, then they utilized these HPNs in the designing of a soft arm that mimicking an elephant trunk in its shape, strength, and flexibility. The end effector position control has been performed, also the soft arm proved its applicability in solving different issues, like Opening a drawer, unscrewing a bottle cap, shifting a gear, opening a door, turning a parallel handwheel, cleaning the glass, and else. Firstly, an open-loop control system has been used by the authors by utilizing the neural network but this method doesn't meet the accuracy requirements, so an estimated hybrid closed-loop control system has been presented, and the third method is a model-free control strategy using Q-learning as the reinforcement learning algorithm. Also, a novel extensor bending pneumatic artificial muscles (EBPAMs) was presented by H. Al-Fahaam *et al* [8] to explain the performance of the proposed actuator a power augmentation and rehabilitation soft glove has been designed, which helps reduce the amount of muscular effort needed to hold and carry things in some disease states, and EMG signals from the muscle were used in open-loop control strategy to perform the simple grasps. The RBO Hand 2 was designed by Raphael Deimel and Oliver Brock, it is a dexterous grasping robotic hand that is compliant and underactuated, this type of continuum actuator design is also called PneuFlex actuators. It's constructed of silicone rubber, polyester fibers, and a polyamide scaffold, and it's pneumatically activated. For computing valve opening times, it uses a basic linear forward model as a control mechanism. The model considers the regulated supply pressure to obtain the desired channel pressure, which corresponds to the intended bending radius or contact force [9]. A different

approach was used by James M. *et al*, by employing a learned differentiable model instead of a precisely prepared finite element method (FEM) simulation to guide the control method. The forward kinematics of a soft robot are in their most basic form, a map from motor angles to the end-effector position, a small feedforward neural network has been trained to link control inputs to the quasi-static end-effector position predictions. Data were collected either in the real world utilizing motion capture to obtain training data for a three-degree-of-freedom soft foam robotic arm or through simulation, and a presentation of the general method that gives a useful foundation for learning the mechanics of a soft robot [10].

According to the literature, many control methods have been developed; however, the ideal technique for modeling and controlling soft robots is still a work in progress. In this article, we contributed by designing several simulation-based control techniques, as well as analyzing and comparing these accomplished control approaches in terms of time-domain characteristics.

II. PNEUMATIC SOFT ACTUATOR

Electromechanical actuators (such as DC, Stepper, and Servo motors) work by combining magnets and wire coils to produce motion, while compressed air energy is converted into mechanical motion by the pneumatic actuation, and the hydraulic actuation is based on the idea of manipulating fluid to generate mechanical motion [11].

Several researchers focused their studies on the development of the McKibben artificial muscle, which is one of the most efficient and widely used fluidic artificial muscles. There are different types of McKibben's muscles, the extension muscle whose length increased with the applied pressure, and the contraction muscle whose length decreased with the applied pressure [4], and the bending muscle which is formed by reinforcing one side of the above previous muscles to prevent them from stretching or contracting respectively. By using A 3D printed thin incompressible reinforcing rod in the contractor muscle, or by using a thread that fixes one side of the extensor muscle. So, the bending behavior can be obtained from the PMA using the proposed techniques [7][6]. The soft actuator must be able to move flexibly while maintaining sufficient force output capability; on the other hand, the soft actuator must be able to maintain stable control in three-dimensional space when subjected to external disturbances [2].

These actuators are small and light, yet they can generate a lot of force. Furthermore, because air is compressible, the actuators are flexible and compliant. On the other hand, the actuator can only produce force in one direction, allowing them to be utilized in an antagonistic pair. This allows for changing stiffness by varying the total pressure in both muscles [12].

A new generation of soft robots that can safely interact with humans has been created using soft actuators. And for these soft actuators, the interaction between the shell and the bladder, the bladder shape altering, and the interaction among the braided threads have all been proven to create hysteresis in their behavior [13].

III. CONSTRUCTION AND OPERATION OF SCPMA

The PMA is typically made up of an inner rubber tube, a braided sleeve, and two plastics (or other solid material) terminals that are connected by cable ties. A tiny hole is located on one of the terminals for actuated air input and output [14]. The pneumatic muscle actuator's basic design is shown in Fig. 1.

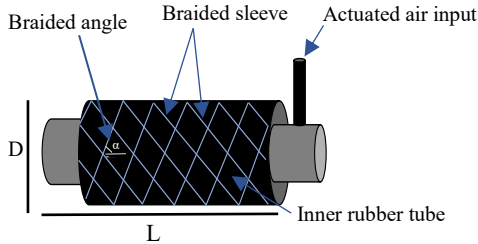


Fig. 1: The pneumatic muscle actuator's basic design.

The rubber tube expands radially and shrinks in length when compressed air is blown into its interior. The inner netting functions as a spring to restore the tube's shape as air leaves the tube., as shown in Fig. 2.

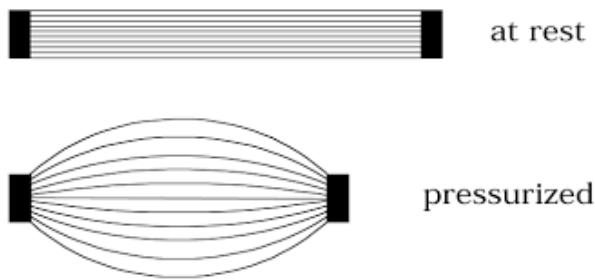


Fig. 2: Soft contraction pneumatic muscle actuator operation.

This reversible physical deformation caused by pneumatic muscle contraction results in linear motion. PMA turns pneumatic power into pulling force and provides several advantages over traditional pneumatic cylinders, including a high force-to-weight ratio, flexible installation options, no mechanical parts, lower compressed air usage, and low cost [15].

The principle operation of the contractor pneumatic muscle can be clearly explained in two scenarios: (a) varying the load with constant air pressure, and (b) fluctuating air pressure at a fixed, attached load. The diameter of the braided sleeve increases as the air pressure rises, and as a result, the diameter of the PMA rises as well, while the actuator length decreases to meet the maximum contraction ratio (ϵ). The contraction ratio expression is given by (1):

$$\text{contraction ratio } (\epsilon) = \frac{L_0 - L}{L_0} \quad (1)$$

where L_0 is the initial length of the actuator and L is the length of the PMA under pressure [3].

Fig. 3 shows the variation of the PMA length with different applied air pressure from (0-5 bar)

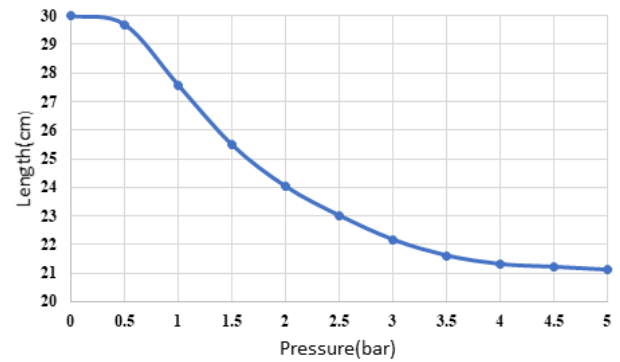


Fig. 3: Length changing of the Soft Contractor Pneumatic Muscle Actuator according to different applied pressure.

The well-known outline of the pneumatic muscle's constitution is seen in Fig. 4, l represents the actuator length, D is the actuator diameter, while c is the length of the braided sleeve thread assuming the mesh material is inextensible, and the number of turns for a single thread represents by n , as well α is the angle formed between the thread and the actuator's long axis, this angle varies depending on the muscle's length, all of these form the geometric constants of the system.

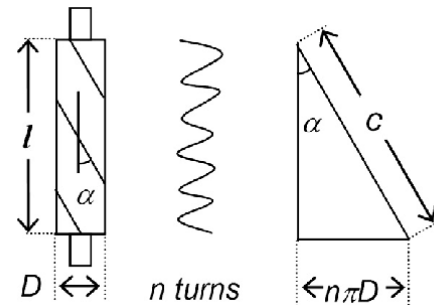


Fig. 4: geometrical representation of the Pneumatic muscle actuator.

IV. MODELING OF THE SCPMA

Many authors have worked on developing a mathematical model that represents the behavior of the pneumatic muscle actuator to figure out how the pneumatic muscle's length, force, and pressure all relate to one another.

According to the muscle length shape in Fig (3). an important and accurate mathematical model was developed [14], the author discovered that the PMA behaves like a sigmoid-type function in mathematics. Additionally, the nominal length L_0 of each muscle ranges between 15 and 40 cm, also it has been researched and documented how muscle length varies with applied pressure. He also demonstrates that the theoretical and experimental results significantly match each other. In view of that, various equations based on the PMA nominal length (L_0) and air pressure (p) were defined. The pneumatic muscle length mathematical model was described in (2) using both (p & L_0), and the parameters values of (2) were evaluated in (3) based on the nominal length of the Pneumatic muscle actuator.

$$L = a + \frac{b}{[1+(\frac{p}{c})^d]^e} - 0.009L_0\sqrt{p} \quad (2)$$

Where:

$$\begin{bmatrix} a \\ b \\ c \\ d \\ e \end{bmatrix} = \begin{bmatrix} 0.4351 & 0 & 0.0183 & -0.0003 \\ 0.5649 & 0 & -0.0183 & 0.0003 \\ -0.0141 & 0 & 0.0031 & -0.00006 \\ 0.5487 & 0 & -0.0136 & 0.00007 \\ 0 & 0.3694 & 0 & 0 \end{bmatrix} \begin{bmatrix} L_0 \\ L_0^{-0.248} \\ L_0^2 \\ L_0^3 \end{bmatrix} \quad (3)$$

V. CONTROLLING OF THE SCPMA

This section discusses the control methods that were used to adjust the position of the soft contraction pneumatic muscle actuator, starting from the most basic ON-OFF controller (also known as bang-bang controllers), PID controller, to the soft computing techniques such as neural network controllers and fuzzy logic controllers. The simulation technique in MATLAB/SIMULINK was used to produce the results theoretically. Two signals were used to perform the experiments, a sinusoidal signal, and a square wave signal.

A. Bang –Bang

A bang-bang controller, also known as the On-Off controller or the hysteresis controller, is a type of discontinuous feedback controller that alternates between two values frequently. This form of the controller is often used to manage a plant that receives a binary input, and due to the simplicity and lower cost of discontinued actuators that operate on the bang-bang principle, such as solenoid valves and relays, over continuous actuators; it could be considered as the most popular type of controller used in the industrial field. [16].

The On-Off control is the simplest form of a controller, turning on when the error is positive and off when the error is zero or negative. There are no intermediate states in an On-Off controller; instead, there are only fully on or entirely off states.

In some cases, such as temperature and pressure control, this type of controller would be ideal due to its simplicity and convenience. It would also be more appropriate for issues involving a control action that is constrained between upper and lower bounds.

In our case, a relay was used to accomplish the control operations on two separate signals that range from 30 to 24 cm which are the step input signal, and the sinusoidal wave signal, firstly the step input signal is used, and we obtained a very accurate response from this simple control strategy with nearly zero steady-state error, as shown in Fig. 5.

On the other hand, an imprecise signal tracking was obtained from the second sinusoidal wave signal by using this bang-bang controller as seen in Fig. 6.

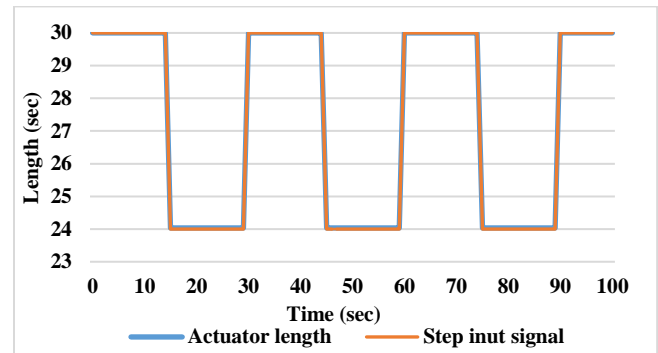


Fig. 5: The response of the Bang-Bang controller for the step input signal.

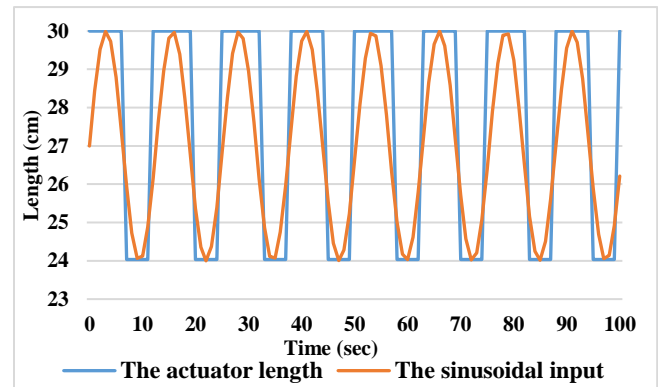


Fig.6: The response of the Bang-Bang controller for the sinusoidal wave signal.

B. PID

The PID controller is the most popular feedback type, conventional controller. PID control systems became the standard tool in many applications when process control became popular in the 1940s. Today, PID control loops represent about 95 percent or more of all control loops in process control; in fact, PI control loops account for the majority of loops [17].

This strategy is especially appropriate when the mathematical model of the system is unknown or it's too sophisticated. The required controller response must be acquired by modifying the parameters of the PID which is depending on the individual application, the tuning procedure is typically applied to improve the overall performance of the system. as well PID employed control loop feedback to perform control actions in industrial and control systems applications. The controller determines the error value by comparing a measured process variable to the desired set point. Then it seeks to reduce or increase the controller's inputs or outputs to get the process variable closer to the set point [18].

The PID controller is made up of three terms: proportional (P), integral (I), and derivative (D). The typical PID controller structure is shown in Fig. 7.

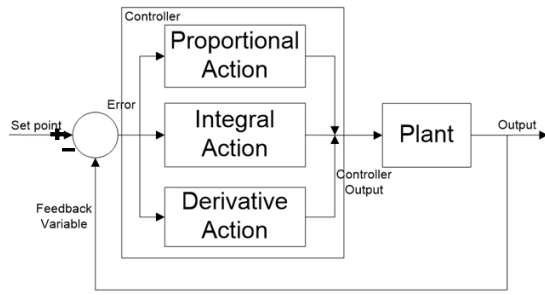


Fig. 7: PID control system block diagram.

The output $u(t)$ of the PID controller, in its ideal form, is the summation of the three terms as indicated in “(4),” -

$$u(t) = k_p e(t) + k_i \int e(t) dt + k_d \frac{d}{dt} e(t) \quad (4)$$

To regulate the contraction length of the SCPMA, a MATLAB Simulink PI controller was created in this section. We noticed that adding the D term causes the controller's response to oscillate to very high values, resulting in an undesirable response, so there is a clear rationale for avoiding adding the derivative (D) term to the PID controller and reducing it to a PI controller. A 30-second step input signal with a 50-pulse width was used. The results in “Fig. 8” were obtained through the trial-and-error method to adjust the parameters of the controller.

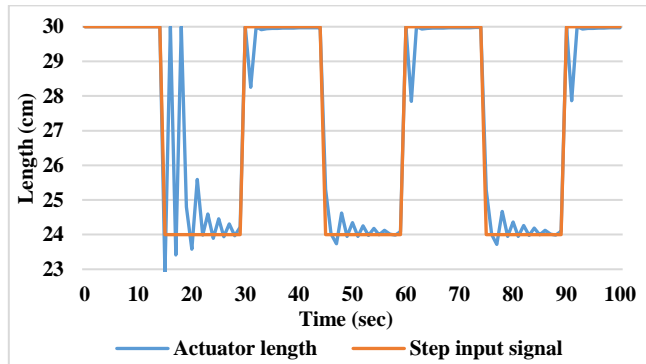


Fig. 8: The response of the PID controller for the step input signal.

After the PI control system received a second input signal in the form of a sinusoidal wave signal; Fig. 9 depicts the controller reaction.

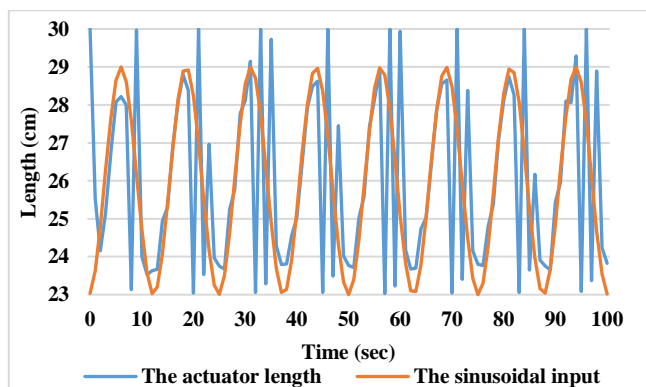


Fig. 9: The response of the PID controller for the sinusoidal wave signal.

C. Neural network

Several distinct types of artificial neural networks (ANNs) have been employed in many applications to try to replicate the way the human brain works and uncover relationships between sets of data [19]. It is also an excellent solution for difficulties with complex and noisy sensor data. Three layers constitute the initial version of the neural network: the input layer, hidden layer, and output layer. As the model becomes more complicated, the number of NN layers will increase.

Different training procedures, such as machine learning algorithms, were employed to train the neural networks. The input signals travel through the hidden layer, the following layer, and lastly to the output layer, which generates the final prediction. ANNs are made up of nodes or neurons, which are extremely related mathematical units. Several parameters (biases and weights) must be tuned to accomplish the control operations; and by modifying the parameters values, a wide range of outputs can be obtained.

The ANN can solve an endless number of complicated jobs. In our example, we employed the Nonlinear Autoregressive Moving Average (NARMA-L2) model, which is a well-known ANN design for prediction and control. The proposed ANN model is used in several process control systems, such as cancer chemotherapy to regiment drug dosage and the magnetic levitation process. Another advantage of this model is that it reduces computation time and memory requirements. Moreover, its mapping capabilities should enable more precise and rapid output planning [20]. feedback linearization controller and NARMAL2 controller are two terms used to describe the ANN controller architecture utilized in this section. When the model has a specific shape (companion form); it is called a feedback linearization controller. In contrast, NARMA-L2 controllers are utilized when the system model can roughly be approximated by the same form [21].

It's a close-to-equilibrium discrete-time nonlinear dynamical system representation. The primary principle of this type of controller is to cancel nonlinearities in order to convert nonlinear system dynamics to linear dynamics. The controller is learned offline and is simply a rearranged version of the neural network's plant model [22].

The output $u(k)$ for the NARMA-L2 NN controller may be described as:

$$u(k) = \frac{y_r(k+1) - f[y_n(k), u_m(k-1)]}{g[y_n(k), u_m(k-1)]} \quad (5)$$

Using neural networks $f(\cdot)$ and $g(\cdot)$ can be approximated. And:

$$y_n(k) = [y(k), \dots, y(k-n+1)]^T \quad (6)$$

$$u_m(k-1) = [u(k-1), u(k-2), \dots, u(k-m)]^T \quad (7)$$

The NARMA-L2 NN-controller was designed using MATLAB Simulink, with a single hidden layer of 5-neurons, two delayed plant input signals, and one delayed plant output signal. 'trainlm' has completed the training procedure for the NN over 100 Epochs. The output signal from the controller is utilized to modify the quantity of compressed air flowing within the PMA to inflate and deflate the bladder to reach the

required length (here between 29-24cm). the suggested NN control system's block diagram is shown in Fig. 10.

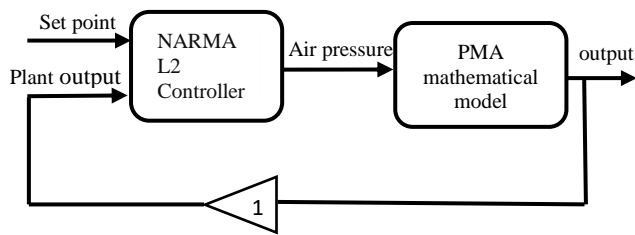


Fig. 10: The NN control system's schematic diagram.

At 0.5 Hz, and for the same sinusoidal wave input signal applied to the controller system, the response in Fig. 11 has better tracking accuracy and fewer signal fluctuation than the PID controller.

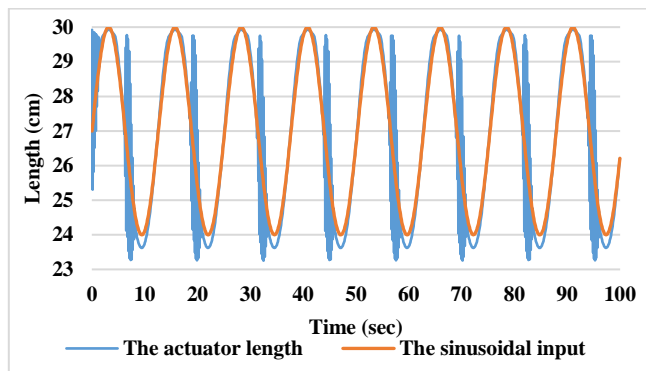


Fig. 11: The response for the NARMA-L2 NN-controller for the sinusoidal wave signal.

The step input signal for 0.5 Hz is used as an additional input signal in Fig. 12 to evaluate the performance of the controller. We can see that the desired signal has resulted in fewer tracking errors.

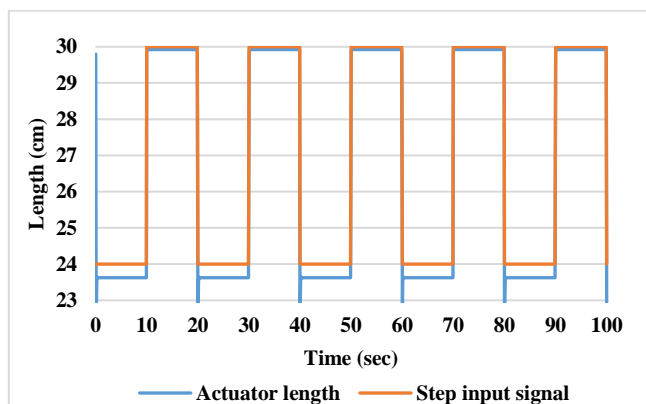


Fig. 12: The response of the NARMA-L2 NN-controller for the step input signal.

D. Fuzzy

In 1965, Lotfi Zadeh created fuzzy logic as development of boolean logic based on the mathematical theory of fuzzy sets, which is a generalization of classical set theory. In other words, the fuzzy set theory includes the classical set theory

as a subset. In the verification of the conditions, the concept of degree has been introduced, this enables things to exist in a state that is not true or false. In addition, the fuzzy logic controller (FLC) increased the amount of flexibility available for dealing with errors and uncertainties. in a variety of difficult challenges [23].

The fuzzy inference system (FIS) is a method for simulating human reasoning, as well as a representation of the knowledge and experience of human operators. The linguistic fuzzy rules are mainly based on human decisions and procedures for solving a specific situation. Even in the presence of parameter variations, the FLC's adaptive and nonlinear nature provided robustness. For complicated, uncertain, and nonlinear systems, it can track desired control actions without the requirement for mathematical models or parameter estimation. [24].

Fuzzification, fuzzy inference, and defuzzification are the three steps that make up FLC. By specifying the membership function for both input and output variables and transforming them into linguistic variables, the fuzzification method is used to transform the in/out crisp variables from classical variables to fuzzy variables in the first stage.

In our example, the membership function was calculated using the set-point (actual muscle length) and the value of the error as inputs to the FLC, and the output is the air pressure value. The fuzzy inference then processes the fuzzy variables to provide the appropriate output; there will be nine fuzzy rules created at this step, these rules indicate the knowledge of an expert in any related application field.

Fig. 13 demonstrates the FIS decisions representation. To achieve the needed control objectives, the defuzzification method should be used to transform the fuzzy outputs back into crisp variables.

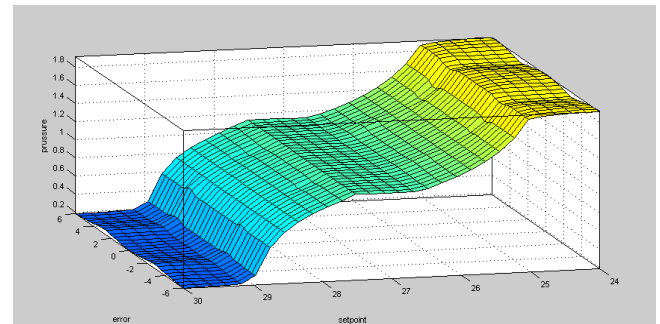


Fig. 13: The fuzzy logic controller rules surface.

After completing the simulation process for the FLC, the outcomes for the step input signal and the sinusoidal wave signal, respectively, are shown in Fig. 14 and Fig. 15. We discovered that the FLC is more adaptable and has a better response than the other controllers, with less fluctuation and steady-state error in the output signal.

Examining the amplitude vs. time characteristics of a measuring signal represents time-domain analysis, which provides the system's behavior over time, allowing predictions and regression models for the signal. And we can see from all of the previous cases for control systems that there is a variation in several time-domain characteristics in this issue. Which is represented by the oscillation in the

output signal or overshoot and undershoot values, as well as the steady-state error.

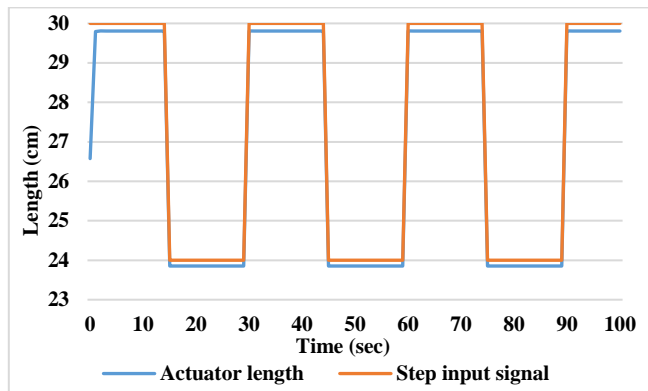


Fig. 14: The response of the fuzzy controller for the step input signal.

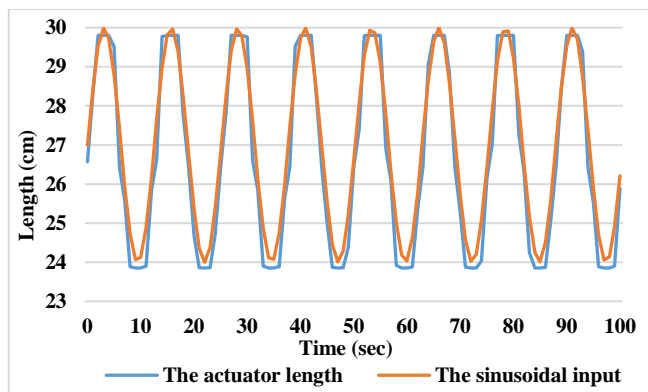


Fig. 15: The response of the fuzzy controller for the sinusoidal wave signal.

For the series of step sine-wave signal inputs that are applied to the controllers, Fig.16 and Fig.17 respectively show the comparison of the different control systems. For the Bang-Bang controller, a very accurate response was accrued from this simple control technique, with nearly zero steady error, no overshoot or undershoot, no oscillation in the

measured signal and the root mean square error (RMSE) was 0.02633.

For the PID controller, an undesired oscillation and steady-state error were existing in the measured signal, undershoot with a value of 1.2 cm before returning to the target position, but with no overshoot and the RMSE value was 0.20803.

For the neural network controller, no oscillation in the output signal, and no overshoot but the controller reaches a point where it is with a steady-state error of about 0.38 and 0.07 and it continues in the same manner, the response also has an undershooting value of 1.6 cm and root mean square error RMSE value is 0.58240.

And for the fuzzy controller, a very accurate response was obtained from this strategy, there is no overshoot, nor oscillation in the measured signal, undershoot of 0.15 cm and the steady-state error is slightly about 0.18 and 0.15 and the root mean square error (RMSE) was found to be 0.17677.

By observing the control systems' responses using the sinusoidal wave signal in Fig. 15 we can see that the measured signal varies for the different control systems too. Starting with the Bang-Bang controller, we will notice a failure to track the desired sinusoidal wave signal, as it is an on-off controller, which means it is not affected by the sinusoidal wave smooth transitions, so the output will take the shape of the square signal. In this case, the RMSE is about 2.03459.

For the PID controller, the oscillation also presents here and the overshoot is about 1 cm but with no undershoot, the steady-state error was also existing and the value of the RMSE is about 3.70030.

For the neural network controller, a little oscillation was existing in the output signal and the steady-state error was approximately about 0.35 cm and the undershoot was 0.7 cm, no overshoot exists and the RMSE is 3.25809.

while for the fuzzy controller, a good tracking for the desired signal was found with nearly no oscillation, no overshoot nor undershoot, a very little steady-state error of 0.15 cm was found and the RMSE is 0.46621.

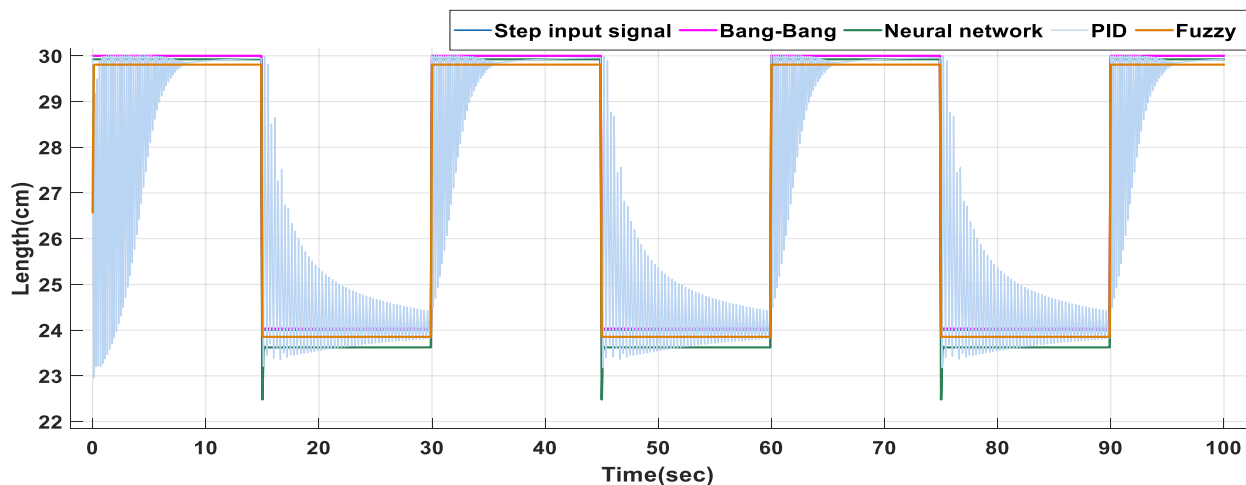


Fig. 16: Comparison of various control systems used with the soft contractor pneumatic muscle actuator (SCPMA) in the case of the step input signal.

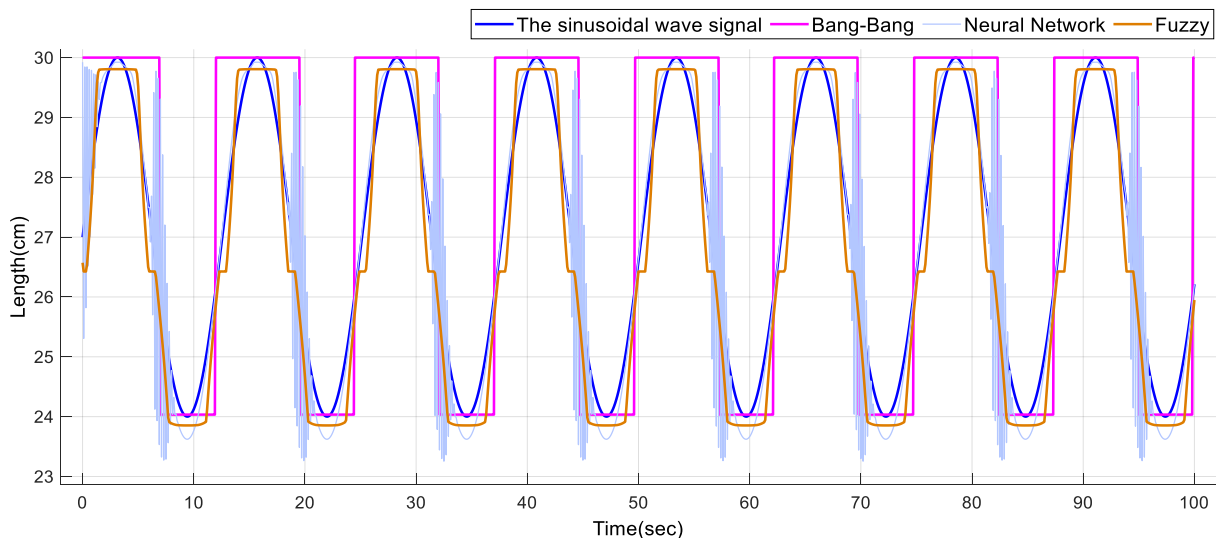


Fig. 17: Comparison of various control systems used with the soft contractor pneumatic muscle actuator (SCPMA) in the case of the sinusoidal wave signal.

VI. CONCLUSIONS

Without a clear comparison ground, determining whether a particular control system is appropriate for a given application is extremely difficult. As a result, the purpose of this paper is to contribute a more systematic approach to assessment.

The actuator dynamics were driven by two input signals: the square wave signal and the sinusoidal wave signal, and a 30 cm to 24 cm length for the soft contraction pneumatic muscle actuator (SCPMA) was achieved using various types of control systems, including Bang-Bang, PID, neural network, and fuzzy controllers. The performance accuracy varied from one controller type to another based on different parameters. Finally, as an open discussion for the research community, particularly in soft robotics, these control techniques can be further developed by combining two of them, resulting in a hybrid system.

Different reference input signals may also be applied to these controllers in the future for further performance validation.

CONFLICT OF INTEREST

There are no competing interests between the authors that are pertinent to this article.

REFERENCES

- [1] D. Rus and M. T. Tolley, "Design, fabrication and control of soft robots," *Nature*, vol. 521, no. 7553, pp. 467–475, 2015.
- [2] H. Jiang *et al.*, "Design, control, and applications of a soft robotic arm," *arXiv Prepr. arXiv2007.04047*, 2020.
- [3] A. Al-Ibadi, S. Nefti-Meziani, and S. Davis, "Efficient structure-based models for the McKibben contraction pneumatic muscle actuator: The full description of the behaviour of the contraction PMA," in *Actuators*, vol. 6, no. 4, p. 32, 2017.
- [4] L. A. T. Al Abeach, S. Nefti-Meziani, and S. Davis, "Design of a variable stiffness soft dexterous gripper," *Soft Robot.*, vol. 4, no. 3, pp. 274–284, 2017.
- [5] A. Al-Ibadi, S. Nefti-Meziani, and S. Davis, "Design, implementation and modelling of the single and multiple extensor pneumatic muscle actuators," *Syst. Sci. Control Eng.*, vol. 6, no. 1, pp. 80–89, 2018.
- [6] A. Al-Ibadi, S. Nefti-Meziani, and S. Davis, "Active soft end effectors for efficient grasping and safe handling," *IEEE Access*, vol. 6, pp. 23591–23601, 2018.
- [7] A. Al-Ibadi, "The Design and Implementation of a Single-Actuator Soft Robot Arm for Lower Back Pain Reduction," *Iraqi J. Electr. Electron. Eng.*, no. 3RD, 2020.
- [8] H. Al-Fahaam, S. Davis, and S. Nefti-Meziani, "The design and mathematical modelling of novel extensor bending pneumatic artificial muscles (EBPAMs) for soft exoskeletons," *Rob. Auton. Syst.*, vol. 99, pp. 63–74, 2018.
- [9] R. Deimel and O. Brock, "A novel type of compliant and underactuated robotic hand for dexterous grasping," *Int. J. Rob. Res.*, vol. 35, no. 1–3, pp. 161–185, 2016.
- [10] J. M. Bern, Y. Schneider, P. Banzet, N. Kumar, and S. Coros, "Soft robot control with a learned differentiable model," in *2020 3rd IEEE International Conference on Soft Robotics (RoboSoft)*, 2020, pp. 417–423.
- [11] F. Taher, J. Vidler, and J. Alexander, "A characterization of actuation techniques for generating movement in shape-changing interfaces," *Int. J. Human-Computer Interact.*, vol. 33, no. 5, pp. 385–398, 2017.
- [12] L. A. T. Al Abeach, *Pneumatic variable stiffness soft robot end effectors*. University of Salford (United Kingdom), 2017.
- [13] C. P. Chou and B. Hannaford, "Measurement and modeling of McKibben pneumatic artificial muscles," *IEEE Transactions on Robotics and Automation*, vol. 12, no. 1, pp. 90–102, 1996. doi: 10.1109/70.481753.
- [14] A. Al-Ibadi, S. Nefti-Meziani, and S. Davis, "Valuable experimental model of contraction pneumatic muscle actuator," in *2016 21st International Conference on*

- Methods and Models in Automation and Robotics (MMAR)*, pp. 744–749, 2016.
- [15] E. Kelasidi, G. Andrikopoulos, G. Nikolakopoulos, and S. Manesis, “A survey on pneumatic muscle actuators modeling,” in *2011 IEEE International Symposium on Industrial Electronics*, pp. 1263–1269, 2011.
- [16] A. Ryniecki, J. Wawrzyniak, and A. A. Pilarska, “Basic terms of process control: the on-off control system,” *Przem. Spożywczy*, vol. 69, no. 11, pp. 26–29, 2015.
- [17] J. Paulusová and M. Dúbravská, “Application of design of PID controller for continuous systems,” *Humusoft. Cz.*, vol. 1, pp. 2–7, 2012.
- [18] A. K. Ho, “Fundamental of PID Control,” *PDHonline Course E*, vol. 331, 2014.
- [19] F. Barkrot and M. Berggren, “Using machine learning for control systems in transforming environments”, Department of Computer and Information Science, Linköping University, 2020.
- [20] S. S. Mokri, H. Husain, W. Martono, A. Shafie, and U. K. M. Bangi, “Real time implementation of NARMA-L2 control of a single link manipulator,” *Am. J. Appl. Sci.*, vol. 5, no. 12, pp. 1642–1649, 2008.
- [21] M. Jibril, M. Tadese, and E. Alemayehu, “Tank Liquid Level Control using NARMA-L2 and MPC Controllers,” *Res. J.*, vol. 12, no. 7, 2020.
- [22] A. Pukrittayakamee, O. De Jesús, and M. T. Hagan, “Smoothing the control action for NARMA-L2 controllers,” in *The 2002 45th Midwest Symposium on Circuits and Systems, 2002. MWSCAS-2002.*, vol. 3, pp. III–III, 2002.
- [23] F. DERNONCOURT, “Introduction to fuzzy logic,” *Massachusetts Inst. Technol.*, vol. 21, pp. 50–56, 2013.
- [24] I. H. Altas and A. M. Sharaf, “A generalized direct approach for designing fuzzy logic controllers in Matlab/Simulink GUI environment,” *Int. J. Inf. Technol. Intell. Comput.*, vol. 1, no. 4, pp. 1–27, 2007.